Stabilization of Isolated Mixed-Valence Trimers in a Novel Nickel Dithiolene Complex with CF_2 Substituents

Olivier J. Dautel and Marc Fourmigué*

Laboratoire Sciences Moléculaires aux Interfaces, CNRS FRE 2068, Institut des Matériaux Jean Rouxel, 2, rue de la Houssinière, BP32229, 44322 Nantes Cedex 3, France

Received December 7, 2000

The preparation of the novel paramagnetic nickel dithiolene complex $Ni(F_2pdt)_2^{-\bullet}$ (F_2pdt^{2-}: 2,2-difluoro-1,3-propanediyldithioethylene-1,2-dithiolate) and its X-ray crystal structure as *n*-Bu_4N^+ salt are described. (*n*-Bu_4N)[$Ni(F_2pdt)_2$] (**2**) crystallizes in the orthorhombic system, space group $Pna2_1$ with $a = 21.379(4)$ Å, $b = 8.9702(18)$ Å, and $c = 18.527(4)$ Å. The radical anions are isolated from each other by the bulky *n*-Bu_4N^+ cations and exhibit a Curie-type magnetic behavior. Two reversible redox waves corresponding to the redox couples $Ni(F_2pdt)_2^{2-/-\bullet}$ and $Ni(F_2pdt)_2^{-\bullet/0}$ are observed at −0.55 and 0.30 V vs SCE, illustrating the electron withdrawing effect of the CF_2 substituents. As a consequence, $(TTF)_3(BF_4)_2$ oxidation of the radical anion does not afford the neutral $Ni(F_2pdt)_2^0$ but a TTF salt formulated as $[TTF]_3[Ni(F_2pdt)_2]_3[CH_2Cl_2]$. It crystallizes in the triclinic system, space group $P\bar{1}$ with $a = 12.330(3)$ Å, $b = 12.726(3)$ Å, $c = 15.706(3)$ Å, $\alpha = 91.10(3)$, $\beta = 110.78(3)$, and $\gamma = 116.01(3)$. Donor and acceptor moieties are organized into $(TTF)_3^{2+}$ and $[Ni(F_2pdt)_2]_3^{2-}$ trimers whose dicationic and dianionic charges have been inferred from the intramolecular bond lengths evolution and the singlet−triplet magnetic behavior. These trimers arrange orthogonally to each other into chess-board-like slabs, characterized by a segregation of the CF_2 fragments and further stabilized by weak C−H···F interactions. Extended Hückel calculations show that only the nickel dithiolene complex trimer actually contributes to the magnetic susceptibility.

Introduction

In our quest for novel electroactive solid-state architectures induced by weak intermolecular interactions[1] (hydrogen bonds,[2] halogen/halogen,[3] and cyano/halogen[4] interactions) between open-shell molecules through the reasoned functionalization (alcohols, phosphonates, carboxylic acids, amides,[5] and halides)[6] of the tetrathiafulvalene (TTF) redox core, we were recently attracted by the strong segregation patterns observed with highly fluorinated molecules.[7] Indeed, perfluorinated alkanes or cycloalkanes do not mix with the usual organic solvents and amphiphilic molecules based on perfluorinated tails lead to the formation of lyotropic liquid crystalline phases.[8] We therefore decided to investigate the structuring role of such a segregation for the elaboration of solid-state materials and introduced a limited number of CF_2 groups on a tetrathiafulvalene core,[9] thus offering a unique opportunity for combining the overlap interaction of open-shell molecules with the nonbonded interactions of the fluorinated moieties. The bis(difluoropropylenedithio)-tetrathiafulvalene[9] (F_4BPDT-TTF) was shown to indeed adopt a layered structure with a full segregation of the aromatic and fluorinated moieties despite the limited number of CF_2 groups.

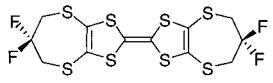

F_4BPDT-TTF

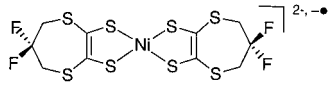

$(F_2pdt)_2Ni^{2-,1-\bullet}$

In this paper we want to extend this structural concept to the solid-state organization of anionic square-planar nickel-dithiolene complexes[10] and explore in those complexes and their salts the competition between the requirements of SOMO−SOMO overlap interactions and those of the fluorine exclusion interactions. We report here on the preparation of the monoanionic, paramagnetic $Ni(F_2pdt)_2^{-\bullet}$ complex (F_2pdt^{2-}: 2,2-difluoro-1,3-propanediyldithioethylene-1,2-dithiolate) and analyze its crystal structure in relation with its magnetic behavior. Its electrocrystallization in the presence of TTF afforded a peculiar mixed-valence salt $[TTF]_3[Ni(F_2pdt)_2]_3[CH_2Cl_2]$, characterized by the presence of fully isolated mixed-valence trimers whose structural and magnetic properties will be described and analyzed.

(1) Desiraju, G. R. *Angew. Chem., Int. Ed. Engl.* **1995**, *34*, 2311−2327.
(2) Jeffrey; G. A.; Saenger, W. In *Hydrogen Bonding in Biological Structures*, Springer-Verlag: Berlin, 1991.
(3) (a) Desiraju, G. R.; Parthasarathy, R. *J. Am. Chem. Soc.* **1989**, *111*, 8725. (b) Price, S. L.; Stone, A. J.; Lucas, J.; Rowland, R. S.; Thornley, A. E. *J. Am. Chem. Soc.* **1994**, *116*, 4910.
(4) (a) Desiraju, G. R.; Harlow, R. L. *J. Am. Chem. Soc.* **1989**, *111*, 6757. (b) Lommerse, J. P. M.; Stone, A. J.; Taylor, R.; Allen, F. H. *J. Am. Chem. Soc.* **1996**, *18*, 3108.
(5) (a) Heuzé, K.; Fourmigué, M.; Batail, P. *J. Mater. Chem.* **1999**, *9*, 2373. (b) Heuzé, K.; Fourmigué, M.; Batail, P.; Canadell, E.; Auban-Senzier, P. *Chem.—Eur. J.* **1999**, *5*, 2971 and references therein.
(6) (a) Batail, P.; Fourmigué, M. Manuscript in preparation. (b) Bryce, M. R. *J. Mater. Chem.* **1995**, *5*, 1481.
(7) (a) *Organofluorine Chemistry: Principles and Commercial Applications*; Banks, R. E., Smart, B. E., Talow, J. C., Eds; Plenum Press: New York, 1994. (b) Riess, J. G. *New J. Chem.* **1995**, *19*, 891.
(8) (a) Turberg, M. P.; Brady, J. E. *J. Am. Chem. Soc.* **1988**, *110*, 7797. (b) Sadtler, V. M.; Giulieri, F.; Krafft, M.-P.; Riess, J. G. *Chem.—Eur. J.* **1998**, *4*, 1952. (c) Rabolt, J. F.; Russel, T. P.; Twieg, R. J. *Macromolecules* **1984**, *17*, 2786. (d) Russel, T. J.; Rabolt, J. F.; Twieg, R. J.; Siemens, R. L.; Farmer, B. L. *Macromolecules* **1986**, *19*, 1135.
(9) Dautel, O. J.; Fourmigué, M. *J. Org. Chem.* **2000**, 65, 6479.
(10) (a) Cassoux, P.; Valade, L.; Kobayashi, H.; Kobayashi, A.; Clark, R. A.; Underhill, A. E. *Coord. Chem. Rev.* **1991**, *110*, 115. (b) Pullen, A. E.; Olk, R.-M. *Coord. Chem. Rev.* **1999**, *188*, 211.

10.1021/ic0013835 CCC: $20.00
Published on Web 03/29/2001

Table 1. X-ray Crystallographic Data

	2	**3**
empirical formula	$C_{26}H_{44}F_4NNiS_8$	$C_{49}H_{36}Cl_2F_{12}Ni_3S_{36}$
fw	761.81	2253.97
temp (K)	150 (2)	293 (2)
λ (Å)	0.71073	0.71073
space group	$Pna2_1$	P-1
a (Å)	21.379(4)	12.330(3)
b (Å)	8.9702(18)	12.726(3)
c (Å)	18.527(4)	15.706(3)
α (deg)	90.00	91.10(3)
β (deg)	90.00	110.78(3)
γ (deg)	90.00	116.01(3)
V (Å)	3553.0(12)	2025.3(7)
Z	4	1
ρ_{calc} (g cm^{-3})	1.424	1.848
μ (mm^{-1})	1.056	1.749
R(F), wR(F^2)	0.0299, 0.0445	0.045, 0.0975

$R(F) = \sum||F_o| - |F_c||/\sum|F_o|$, $wR(F^2) = [\sum[w(F_o^2 - F_c^2)^2]/\sum[w(F_o^2)^2]]^{1/2}$.

Experimental Section

Reagents and Procedures. Preparation of 4,5-(2,2-difluoro)-propylenedithio-2-oxo-1,3-dithiole **2** was previously described.[9] $(TTF)_3(BF_4)_2$ was prepared by literature methods.[11] All solvents were dried by standard techniques prior to use. All reactions were carried out under N_2 with standard Schlenk techniques unless otherwise stated.

[*n*-Bu$_4$N][Ni(F$_2$pdt)$_2$] (2). A sodium methylate solution, prepared by dissolution of metallic sodium (180 mg, 7,83 mmol, 4 equiv) in dry methanol (20 mL), was added dropwise, with vigorous stirring, to a suspension of the dithiocarbonate **1** (1 g, 3.8 mmol, 2 equiv) in dry methanol (90 mL). The reaction was allowed to process for 2 h until complete dissolution of **2** was achieved. To the resulting brown-green solution was slowly added $NiCl_2$ (250 mg, 1.95 mmol, 1 equiv). The mixture was stirred for 6 h while the resulting solution turned dark-brown. Insoluble materials were filtered off and Bu_4NBr (1.76 g, 4.75 mmol, 2.5 equiv) dissolved in a minimal quantity of methanol was added, after which air was bubbled for 15 min. Most of the solvent was distilled off under vacuum to reduce the volume to 50 mL so that a microcrystalline black precipitate formed. This solid was collected by filtration and purified by recrystallization from acetone/2-propanol (1:3) to give black triangles of **1** (500 mg, 34%): mp 153 °C; IR (KBr) 1473 (m), 1462 (m), 1387 (s), 1285 (m), 1258 (s), 1103 (m), 1071 (s), 1010 (s), 863 (m), 822 (m), 736 (m), 484 (m), 430 cm^{-1}. Anal. Calcd for $NiC_{26}H_{44}F_4NS_8$ (761.857): C, 40.99; H, 5.82; F, 9.97; N, 1.84; S, 33.67. Found: C, 41.01; H, 5.81; F, 9.91; N, 1.83; S, 33.25.

[TTF]$_3$[Ni(F$_2$pdt)$_2$]$_3$[CH$_2$Cl$_2$]. *By electrocrystallization*: TTF (6 mg) was introduced in the anodic compartment of an electrochemical cell containing **2** (15 mg) as electrolyte in a 1:1 mixture of CH_3CN and CH_2Cl_2. Galvanostatic oxidation (1 μA cm^{-2}) at 20 °C afforded black crystals on the anode which were harvested after 20 days. *By diffusion*: CH_3CN (1 mL) solutions of $(TTF)_3(BF_4)_2$ (10 mg) and **2** (10 mg) were allowed to diffuse into each other through pure CH_2Cl_2 (1 mL) first introduced at the bottom of a U-shaped tube. Crystals were collected after 2 weeks and washed with pure CH_2Cl_2.

X-ray Crystallographic Studies. Table 1 summarizes the crystallographic details about data collection and structure refinement. Data were collected on an Imaging Plate Diffraction System (Stoe-IPDS) with graphite-monochromatized Mo Kα radiation (λ = 0.71073 Å). Structures were solved by direct methods using SHELXS-86 and refined by the full-matrix least-squares method on F^2, using SHELXL-93 (G. M. Sheldrick, University of Göttingen, 1993) with anisotropic thermal parameters for all non-hydrogen atoms. The hydrogen atoms were introduced at calculated positions (riding model) with C_{sp2}−H and C_{sp3}−H distances of 0.93 and 0.97 Å respectively. Crystallographic data (excluding structure factors) for **2** and **3** have been deposited with the Cambridge Crystallographic Data Center as supplementary publication no. CCDC 160524 and 160525. Copies of the data can be obtained free of charge on application to the director, CCDC, 12 Union Road, Cambridge CB2 1EZ, UK (Fax: int code + (1223) 336-033. E-mail: deposit@ccdc.cam.ac.uk.).

Extended-Hückel Calculations. The tight-binding band structure calculations[12] were of the extended Hückel type.[13] A modified Wolfsberg−Helmholtz formula was used to calculate the nondiagonal $H_{\mu\nu}$ values.[14] Double-ζ orbitals for C, S, Ni, and F were used.

Magnetic Measurements. Magnetic susceptibility measurements were performed on a Quantum Design MPMS-2 SQUID magnetometer operating in the range 4−300 K at 25 000 G with polycrystalline samples of **2** and **3**. Data were corrected for sample holder contribution and Pascal diamagnetism.

Scheme 1

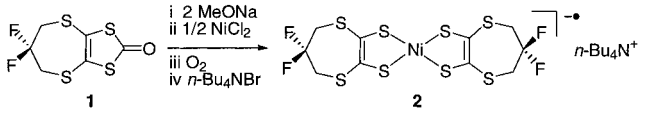

1 **2**

Table 2. Cyclic Voltammetry Data for (*n*-Bu$_4$N)[Ni(F$_2$pdt)$_2$] (**2**) and Reference Compounds (In *V* vs SCE, In CH_3CN with 0.1 M *n*-Bu_4NPF_6 at 100 mV s^{-1})

complex	$E^{1/2}$ (−1 → −2)	$E^{1/2}$ (−1→ 0)	ref
$Ni(F_2pdt)_2^{n-}$	−0.55	+0.30	this work
$Ni(pdt)_2^{n-}$	−0.71	+0.16	15
$Ni(dddt)_2^{n-}$	−0.69	+0.06	15
$Ni(dmit)_2^{n-}$	−0.13	+0.22	17

Results and Discussion

A Novel Paramagnetic Nickel Dithiolene Complex. Reaction of the dithiocarbonate[9] **1** with 2 equiv of MeONa in MeOH followed by addition of $NiCl_2$ afforded the dianionic $Ni(F_2pdt)_2^{2-}$, which was oxidized by air bubbling to the radical anion before being precipitated as its tetrabutylammonium salt upon addition of *n*-Bu_4NBr (Scheme 1). Recrystallization from acetone/2-propanol afforded (*n*-Bu$_4$N)[Ni(F$_2$pdt)$_2$] (**2**) as black platelets in 34% yield. Cyclic voltammetry experiments show that **2** can be reversibly oxidized or reduced (Table 2) to the corresponding neutral $[Ni(F_2pdt)_2]^0$ (**3**) or the dianionic $[Ni(F_2pdt)_2]^{2-}$, respectively.

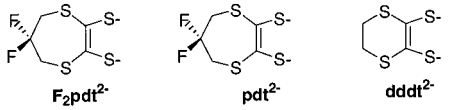

When compared with the nonfluorinated analogue $Ni(pdt)_2^{-\bullet}$,[15,16] both potentials are shifted toward slightly more anodic values, demonstrating the limited but still sizable electron attracting effect of the fluorine functionalization which adds to that of the ethylene/propylene substitution: we note indeed that $Ni(pdt)_2^-$ oxidizes at higher potentials than $Ni(dddt)_2^-$. As a consequence, the redox behavior of the couple $[Ni(F_2pdt)_2]^{0/-1}$ differs only slightly from that of the prototypical $Ni(dmit)_2^{0/-1}$ system.[15] This is all the more interesting since both systems lie close to the $TTF^{0/+1}$ redox potential (0.33 V vs SCE), a very attractive feature at the origin of the stabilization of mixed-valence in the superconducting $(TTF)(Ni(dmit)_2)_2$ salts.[17,18] It

(11) Wudl, F. *J. Am. Chem. Soc*. **1975**, 97, 1962−1963.
(12) Whangbo, M.-H.; Hoffmann, R. *J. Am. Chem. Soc*. **1978**, *100*, 6093.
(13) Hoffmann, R. *J. Chem. Phys*. **1963**, *39*, 1397.
(14) Ammeter, J. H.; Bürgi, H.-B.; Thibeault, J.; Hoffmann, R. *J. Am. Chem. Soc*. **1978**, *100*, 3686.
(15) Kato, R.; Kobayashi, H.; Kobayashi, A.; Sasaki, Y. *Bull. Chem. Soc. Jpn*. **1986**, *59*, 627.
(16) Bereman, R. D.; Lu, H. *Inorg. Chim. Acta* **1993**, *204*, 53.
(17) Brossard, L.; Bousseau, M.; Valade, L.; Cassoux, P. *C. R. Acad. Sci., Sér. 2* **1986**, *302*, 205.

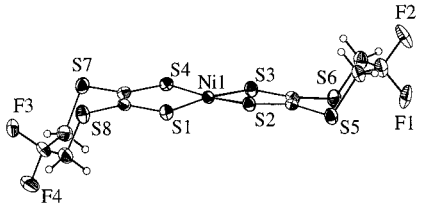

Figure 1. ORTEP view of the $Ni(F_2pdt)_2^{-\bullet}$ radical in its *n*-Bu_4N^+ salt. Ellipsoids are represented at the 50% probability level.

is therefore hoped that TTF salts of $Ni(F_2pdt)_2^-$ might similarly exhibit a mixed-valence state (see below).

(*n*-Bu_4N)[$Ni(F_2pdt)_2$] (**2**) crystallizes in the orthorhombic system, space group $Pna2_1$ with one anion and one cation in general position in the unit cell. The anionic $Ni(F_2pdt)_2^{-\bullet}$ adopts a chair conformation (Figure 1), the nickel is coordinated to the four sulfur atoms of the ligands with a mean Ni−S distance of 2.150(1) Å (Table 3) in a slightly distorted square-planar geometry with a dihedral angle of 9.36(6)° between the two five-membered metallacycles. Other bond distances and angles compare with those described for the analogous nonfluorinated analogues (Table 3). In the solid state, the nickel complexes appear to be essentially isolated from each other by the bulky tetra(*n*-butyl)ammonium cations since the shortest intermolecular S···S distance amounts to 3.957 Å, far above the sum of the S van der Waals radii. Also, the shortest fluorine/fluorine intermolecular distances are far above the $\sum_{vdW}$(F···F) value (2.95 Å), and no specific segregation effects are observed here. The temperature dependence of the magnetic susceptibility of **2** exhibits a Curie−Weiss behavior in the whole temperature range with $\mu_{eff} = 1.806\ \mu_B$, close to the $S = {}^1/_2$ value of 1.73 μ_B and a Curie−Weiss constant θ of −2.5 K, confirming the quasi-absence of any anion−anion interaction in the solid state.

The preparation of this novel paramagnetic dithiolene complex offers numerous opportunities for the elaboration of conducting or magnetic salts if faced with different countercations, be they also diamagnetic as Me_4N^+ or *n*-Bu_4N^+ or paramagnetic as $TTF^{+\bullet}$ or ferricinium.[10] We accordingly performed several electrooxidation experiments with **2** and report here on our first results with $TTF^{+\bullet}$ as countercation.

Mixed-Valence Organic and Inorganic Trimers. The electrocrystallization of TTF in the presence of **2** as electrolyte afforded black plates on the anode. Crystals were harvested on the electrode after one week, and the X-ray crystal structure resolution revealed the formation of a 1:1 salt, or better said a 3:3 salt with dichloromethane inclusion, formulated as $[TTF]_3[Ni(F_2pdt)_2]_3[CH_2Cl_2]$ (**3**). The same compound was also obtained, in larger quantities, by chemical oxidation of **2** with $(TTF)_3(BF_4)_2$ in a U-shaped diffusion cell. It is worth noting here that the similar $(TTF)_3(BF_4)_2$ oxidation of the nonfluorinated analogue, $Ni(pdt)_2^-$, which oxidizes at lower potential,[15] was reported to afford, instead, the corresponding neutral complex $Ni(pdt)_2^0$ rather than a TTF salt.[19] As anticipated above, the higher oxidation potential of **2** effectively allows for the isolation of a $TTF^{+\bullet}$ salt. Compound **3** crystallizes in the triclinic system, space group $P\bar{1}$ (Figure 2). Two crystallographically independent TTF molecules are found, one on an inversion center (noted TTF_A) and one in general position (noted TTF_B), giving rise to a trimeric motif. Similarly, two crystallographically independent $Ni(F_2pdt)_2$ molecules are found, one on an inversion center (noted Ni_A) and one in general position (noted Ni_B), giving rise also to a trimeric motif. Within the TTF trimers (Figure 3), molecules are almost eclipsed with a short plane-to-plane distance (3.485(2) Å), indicative of a possible stabilization of the trimer through HOMO−HOMO overlap interaction of open-shell species (see below). The nickel trimer's geometry (Figure 4) is highly reminiscent of that observed within the stacks of the isosteric neutral fluorinated donor molecule F_4BPDT-TTF[9] but limited here to three molecules. The complexes adopt, indeed, a chair conformation with a plane-to-plane distance (3.615 Å) far shorter than that observed in F_4BPDT-TTF (4.094(8) Å),[9] another indication of a possible stabilization of the open-shell complexes through overlap interaction within each trimer. The fluorine atoms are at van der Waals contacts (2.914 Å) while C−H···F "hydrogen bonds" are identified, characterized with short H···F distances and a tendency to linearity, as illustrated in Figure 5 where the C−H···F angles are plotted against the H···F distances. Such weak hydrogen bonds have been unambiguously identified in fluoroaromatics[20,21] as well as in the structure of the neutral F_4BDT-TTF, they find here their origin in the activation of the methylenic groups located α to the electron-withdrawing CF_2 moieties. Note however that these hydrogen bonds lie somewhat away from the mean θ(C−H··F) vs d(H··F) evolution obtained for fluoroaromatics[20] and F_4BPDT-TTF (Figure 5), a possible consequence of the competing overlap interactions. In the solid state, a two-dimensional segregation of the fluorinated moieties is also observed at $z = 0$ (Figure 6), further stabilized by C−H···F hydrogen bonds at the fluorine/fluorine interface. The TTF trimers arrange between the nickel trimers, with their molecular plane almost perpendicular to the nickel complexes mean planes, giving rise to an unprecedented chess board-like structural organization where each trimer, organic or metallic, is isolated from its congeners by four trimers of different nature.

One crucial point to be addressed here is the actual electronic state of the TTF and the $Ni(F_2pdt)_2$ moieties in **3** which can be described either as a fully ionic salt involving only the radical species $TTF^{+\bullet}$ and the reduced $Ni(F_2pdt)_2^{-\bullet}$, i.e., $[TTF^{+\bullet}]_3[Ni(pdt)_2^{-\bullet}]_3[CH_2Cl_2]$, or as a fully neutral compound with the unoxidized TTF and an oxidized $[Ni(F_2pdt)_2]^0$ or as an intermediate mixed-valence state. Analysis of the bond lengths within the two moieties as well as magnetic susceptibility measurements combined with extended Hückel calculations of the intermolecular interactions within each trimer will allow us to answer this question. As seen in Table 4, the lengthening of the central C=C bond (noted *a*) and concomitant shortening of the C−S bonds (noted *b*) upon TTF oxidation is observed to a larger extent in TTF_A than in TTF_B, the geometrical features of the former being close to those of a fully oxidized $TTF^{+\bullet}$ cation radical. A more quantitative estimate of the degree of charge transfer in both TTF molecules can be obtained from numerical correlations established by Umland between $r = a/b$ or $\delta = a - b$ and the averaged charge q.[22] Both correlations afford here $q_r = 1.04(2)$, $q_\delta = 1.03(8)$ for TTF_A, and $q_r = 0.30(2)$, $q_\delta = 0.32(2)$ for TTF_B. Accordingly, the TTF trimers can be tentatively described as dicationic, i.e., formally $(TTF\_B)^{+0.5}(TTF\_A)^{+1}(TTF\_B)^{+0.5}$. Bond lengths within the

(18) (a) Canadell, E.; Rachidi, I. E. I.; Ravy, S.; Pouget, J.-P.; Brossard, L.; Legros, J.-P.; *J. Phys. (Paris)* **1989**, *50*, 2967. (b) Canadell, E.; Ravy, S.; Pouget, J.-P.; Brossard, L. *Solid State Commun*. **1990**, *75*, 633.

(19) Geiser, U.; Tytko, S. F.; Allen, T. J.; Wang, H. H.; Kini, A. M.; Williams, J. M. *Acta Crystallogr*. **1991**, *C47*, 1164.

(20) Thalladi, V. R.; Weiss, H.-C.; Bläser, D.; Boese, R.; Nangia, A.; Desiraju, G. R. *J. Am. Chem. Soc*. **1998**, *120*, 8702.

(21) (a) Dai, C.; Nguyen, P.; Marder, T. B.; Scott, A. J.; Clegg, W.; Viney, C. *Chem. Commun*. **1999**, 2493. (b) Bats, J. W.; Parsch, J.; Engels, J. W. *Acta Crystallogr*. **2000**, *C56*, 201.

(22) Umland, T.; Allie, S.; Kulhmann, T.; Coppens, P. *J. Phys. Chem*. **1988**, *92*, 6456.

Table 3. Geometrical Characteristics of the Nickel Dithiolene Complexes in the Different Compounds

complex	Ni−S (Å)	C−S_{endo} (Å)	C═C (Å)	C−S_{exo} (Å)	S−Ni−S (deg)
$[Ni(F_2pdt)_2]^{1-}$ in **2**	2.150(1)	1.735(4)	1.346(5)	1.768(4)	91.69(4)
Ni_A in **3**	2.124(2)	1.693(8)	1.393(7)	1.742(5)	90.98(5)
Ni_B in **3**	2.142(2)	1.726(8)	1.367(7)	1.748(5)	92.08(5)

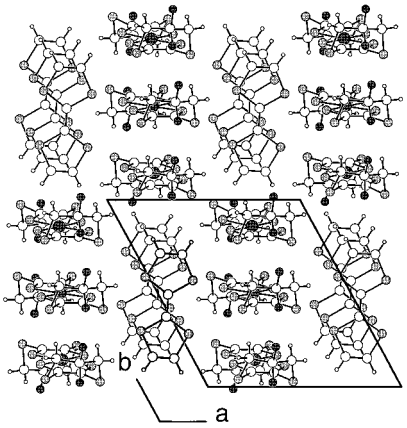

Figure 2. A projection view (along the *c* axis) of the unit cell of $[TTF]_3[Ni(F_2pdt)_2]_3[CH_2Cl_2]$ (**3**) showing the cationic and anionic trimers (Ni and F atoms in dark gray, S atoms in light gray).

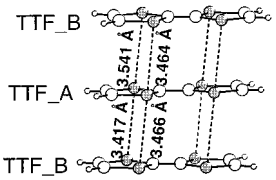

Figure 3. A detail of the cationic (TTF_B)·(TTF_A)·(TTF_B) trimer in **3**. The shortest S···S contacts are indicated as dotted lines (S atoms in light gray).

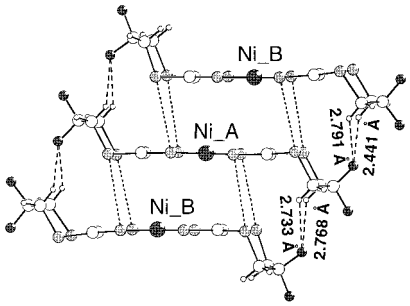

Figure 4. A detail of the anionic (Ni_B)·(Ni_A)·(Ni_B) trimer in **3** (see text). The shortest S···S contacts are indicated as dotted lines, the shortest C−H···F contacts as dashed lines. (Ni and F atoms in dark gray, S atoms in light gray)

$Ni(F_2pdt)_2$ moieties are collected in Table 3. A shortening of the C−S_{endo} bonds and concomitant lengthening of the C═C bonds strongly affect Ni_B while Ni_A geometry compares with that of the anionic $Ni(F_2pdt)_2^{-\bullet}$ in its *n*-Bu_4N^+ salt. Accordingly, the nickel trimer can be tentatively described as dianionic with the $[Ni\_B]^{-0.5}[Ni\_A]^{-1}[Ni\_B]^{-0.5}$ charge repartition and the salt then writes as $[TTF]_3^{2+}[Ni(F_2pdt)_2]_3^{2-}[CH_2Cl_2]$.

As a consequence of this charge repartition, the electron occupancy of the molecular orbitals derived from the three TTF SOMO in the TTF trimer, and the three $Ni(F_2pdt)_2$ SOMO in the nickel dithiolene trimers, leads, as illustrated in Figure 7, to a situation where both organic and inorganic trimers would be closed-shell and therefore diamagnetic, if Δ_{TTF} and Δ_{Ni} are both large enough when compared with *kT*. SQUID susceptibility measurements were performed between 4 and 300 K. The magnetic susceptibility (Figure 8) exhibits a maximum at 45 K

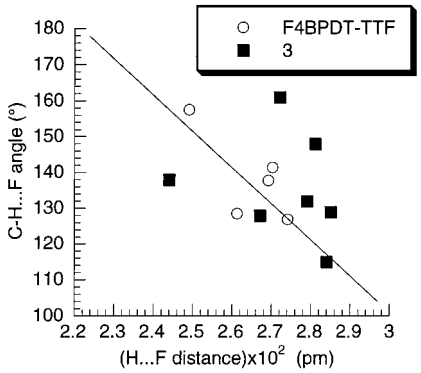

Figure 5. A scatterplot of C−H···F angles vs H···F distances in **3.** The straight line refers to the tendency observed in fluoroaromatics[20] as well as in the neutral F_4BPDT-TTF.

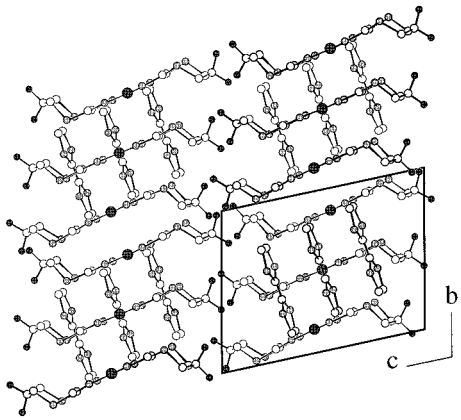

Figure 6. A projection view of **3** along the *a* axis showing the fluorine segregation (Ni and F atoms in dark gray, S atoms in light gray). Note also the orthogonally oriented dicationic and dianionic trimers.

Table 4. Intramolecular TTF Bond Lengths in Different Oxidation States

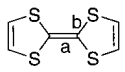

	oxidation state	*a*	b_{av}	ref
TTF^0	0	1.349(3)	1.757(2)	*a*
(TTF)(TCNQ)	0.59	1.369(4)	1.743(4)	*b*
$(TTF)(I_3)$	1	1.382(7)	1.719(8)	*c*
$(TTF)(ClO_4)$	1	1.403(14)	1.713(9)	*d*
TTF_A in **3**	x_1	1.393 (15)	1.715 (7)	*e*
TTF_B in **3**	x_2	1.348 (11)	1.736 (6)	*e*

[a] Cooper, W. F.; Kenney, N. C.; Edmonds, J. W.; Nagel, A.; Wudl, F.; Coppens, J. *J. Chem. Soc., Chem. Commun*. **1971**, 889−890. [b] Kistenmacher, T. J.; Philips, T. E.; Cowan, D. O. *Acta Crystallogr*. **1974**, *B30*, 763−768. [c] Teiltelbaum, R. C.; Marks, T. J.; Johnson, C. K. *J. Am. Chem. Soc*. **1980**, *102*, 2986−2989. [d] Yakushi, K.; Nishimura, S.; Kuroda, H.; Ikemoto, I. O. *Acta Crystallogr*. **1980**, *B36*, 358−363. [e] This work.

together with a Curie tail at low temperatures. This activated behavior can be fitted with the Bleaney−Bower law[23] for *one*

(23) Bleaney, B.; Bowers, K. D. *Proc. R. Soc. London, Ser. A* **1952**, *214*, 451. (b) Kahn, O. In *Molecular Magnetism*; VCH Publishing Inc.: New York, 1993.

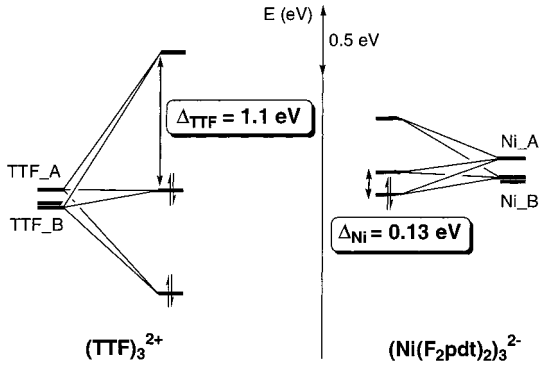

Figure 7. An energy diagram (Extended Hückel calculations) for the $(TTF)_3^{2+}$ and the $[Ni(F_2pdt)_2]_3^{2-}$ moieties. Note the energy differences Δ_{TTF} and Δ_{Ni}.

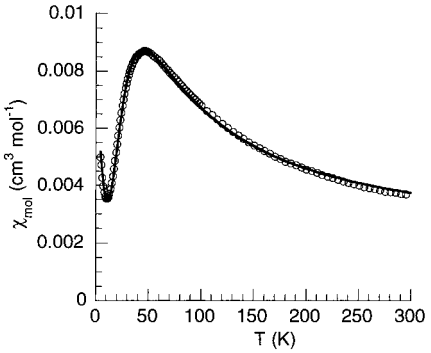

Figure 8. Temperature dependence of the magnetic susceptibility of $[TTF]_3[Ni(F_2\text{-}pdt)_2]_3[CH_2Cl_2]$ (**3**). The solid line is a fit line to the singlet−triplet law, together with a low-temperature Curie tail, $\chi_{mol} = C/T + Ng^2\beta^2/[kT(3 + e^{-J/kT})]$.

singlet−triplet together with a Curie tail, $\chi = C/T + 2Ng^2\beta^2/[kT(3 + e^{-J/kT})]$, with $J/k = -73.8$ K (-51.3 cm^{-1}) and $C = 1.5\ 10^{-2}$ cm^3 K mol^{-1} (i.e., 4% isolated magnetic defects). The contribution of only one singlet−triplet to the susceptibility shows that only one of the dicationic or dianionic trimers contributes to the total magnetic susceptibility for $T < 300$ K. Extended Hückel calculations for each of the donor and acceptor trimer (Figure 7) show that the singlet−triplet excitations, characterized in a crude approximation by the energy differences $\Delta_{TTF} = 1.1$ eV and $\Delta_{Ni} = 0.13$ eV, are expected to occur at much higher temperatures in the TTF trimer. Accordingly, we postulate that the latter is essentially diamagnetic while the singlet−triplet magnetic signature is attributable to the Ni trimers. Furthermore, in a Hubbard model, the antiferromagnetic J value is directly related to Δ, or better the overlap interaction[24] β via $|J| = \beta^2/U$ where U is the on-site Coulomb repulsion, considered to be around to 1 eV in those organic materials. We deduced a calculated J_{calc} value of -95 K, close indeed to the experimental -74 K value deduced from the magnetic data.

The trimeric solid-state association identified here in **3** differs strikingly from the structural motifs usually found in the TTF salts of square-planar metal dithiolene complexes. Besides the conducting stacks or slabs observed with the $M(dmit)_2$ salts (M = Ni, Pt, Pd),[10] other dithiolene complexes most often crystallize with fully oxidized dicationic $(TTF^{+\bullet})_2$ dimers,[25] mixed-valence $(TTF)_2^{+\bullet}$ dimers,[26] or in alternated TTF·complex·TTF·complex... chains.[27] The rare trimeric structure found here can only be compared with that of $(TTF)_3^{2+}(SnCl_6)^{2-}$ where mixed-valence dicationic trimers are also organized orthogonally to each other.[28] In this salt, however, the smaller $SnCl_6^{2-}$ anions do not hinder direct overlap between trimers and accordingly a spin delocalization and a semiconducting behavior. In **3**, the paramagnetic nickel trimers are fully isolated from each other as if they were diluted in a diamagnetic matrix, allowing for the observation of the individual singlet−triplet behavior of the mixed-valence trimeric species. The stabilization of such trimers with a sizable overlap interaction between complexes within each trimer indicates that this system, despite the bulky and nonplanar $CH_2CF_2CH_2$ substituents, is able to sustain mixed-valence and hence a possible conducting behavior in the presence of adapted counteranions. The fluorine segregation plays a limited role in those salts, probably because of its "dilution" with the large n-Bu_4N^+ or $TTF^{+\bullet}$ cations. In that respect, smaller countercations such as Me_4N^+ or Me_3NH^+ might provide stronger intermolecular interactions between the fluorinated radical anions. Inorganic cations such as the alkali metal ions (A^+) might also be of interest since they are known to form specific C−F···A^+ interactions in the solid state.[29] Work is in progress along those lines.

Acknowledgment. We thank the CNRS and the Région Pays de Loire for financial support (to O.J.D.).

Supporting Information Available: Tables of crystal data, positional and thermal parameters, and bond lengths and angles for **2** and **3** in CIF format. This material is available free of charge via the internet at http://pubs.acs.org.

IC0013835

(24) Whangbo, M.-H.; Williams, J. M.; Leung, P. C. W.; Beno, M. A.; Emge, T. J.; Wang, H. H. *Inorg. Chem.* **1985**, *24*, 3500.

(25) Kasper, J. S.; Interrante, L. V.; Secaur, C. A. *J. Am. Chem. Soc.* **1975**, *97*, 890. (b) Schultz, A. J.; Wang, H. H.; Soderholm, L. C.; Sifter, T. L.; Williams, J. M.; Bechgaard, K.; Whangbo, M.-H. *Inorg. Chem.* **1987**, *26*, 3757. (c) Geiser, U.; Schultz, A. J.; Wang, H. H.; Beno, M. A.; Williams, J. M. *Acta Crystallogr.* **1988**, *C44*, 259. (d) Takahashi, M.; Robertson, N.; Kobayashi, A.; Becker, H.; Friend, R. H.; Underhill, A. E. *J. Mater. Chem.* **1998**, *8*, 319.

(26) Mahadevan, J. *Crystallogr. Spectrosc. Res.* **1986**, *16*, 159.

(27) Kasper, J. S.; Interrante, L. V. *Acta Crystallogr.* **1976**, *B32*, 2914.

(28) Kondo, K.; Matsubayashi, G.; Tanaka, T.; Yishioka, H.; Nakatsu, J. *J. Chem Soc., Dalton Trans.* **1984**, 379.

(29) Plenio, H. *Chem. Rev.* **1997**, *97*, 3363.